This manuscript is a pre peer-review version. The final version will be posted in IEEE database after the conference.

# Parallel Pick and Place Using Two Independent Untethered Mobile Magnetic Microgrippers

Jiachen Zhang, Mohammad Salehizadeh, Eric Diller

***Abstract*— Untethered mobile microgrippers exhibit flexibility and agility in small and constrained environments as precise and accurate robotic end-effectors, with promising potential applications in cell manipulation and microassembly. Here, we propose the first scheme to independently and simultaneously position two microgrippers on a horizontal plane for parallel targeted cargo delivery using a single global input. The separation and orientation of the two-microgripper pair are modulated by the local magnetic interactions between the two microgrippers, which are governed by a global magnetic field. The microgripper action of grasping or releasing cargoes is fully controlled by the global magnetic field without requiring additional thermal, chemical, or other stimuli. Thus, the proposed strategy only requires a single input, i.e., a global magnetic field, to control two microgrippers and therefore is simple to implement and fast-acting. As a demonstration, two microgrippers are maneuvered by a global magnetic field to pick up two cargoes and deliver them to their respective destinations. The parallel operation of two microgrippers can potentially double the overall throughput and enable the tasks that require team cooperations.**

***Keywords:*** **magnetic microgripper, multi-agent control at microscales, soft robotics, targeted cargo delivery**

## I. Introduction

Microgrippers are developed as submillimeter robotic end-effectors to perform tasks in small and/or enclosed environments, with the level of precision and accuracy that cannot be achieved by manual operations. The flexibility and agility exhibited by untethered mobile microgrippers make their kind an enabling tool in cell manipulation, targeted therapy, minimally invasive surgery, and microassembly [1]. Various microgrippers have been proposed, characterized, and controlled, which can be categorized into either microelectromechanical systems (MEMS) [2]–[4] or soft elastic microrobots [1], [5]. Randhawa et al. devised a metallic microgripper that responds to chemical stimuli [4]. Leong et al. presented a multiple-layer microgripper that can be remotely triggered by temperature changes and chemicals [6]. Pacchierotti et al. in [7] employed a haptic interface to navigate and manipulate stimuli-responsive soft grippers by human users. Scheggi et al. in [8] used ultrasound imaging technique to detect grippers in situation where visual feedback can not be provided via cameras.

Among many proposed strategies, the magnetic actuation of microrobots becomes a common choice because it can be miniaturized, the field can penetrate most materials, remotely generate both forces and torques on magnetic materials, and it is easy and safe to generate and manipulate [9]. In our previous research, we presented the first three-dimensional (3D) microgripper that is solely controlled by a single global magnetic field [5], and built a feedback controller for it in autonomous 3D pick-and-place tasks [10]. This microgripper is faster compared with the previous microgrippers that require thermal or chemical stimuli besides the magnetic actuation.

Controlling a team of robots in one task can remarkably increase the efficiency and throughput. Besides, certain sophisticated tasks can only be performed by a team of cooperative robots. Controlling multiple microrobots is difficult because their small sizes prevent them from carrying onboard electronics [9]. Thus, multiple microrobots are often operated as an undifferentiated group, such as the $\mu$-grippers in [11] that are randomly scattered to the workspace and then closed by temperate changes. A more challenging goal is to obtain distinct behaviors from each microrobot within a team. To this end, a variety of approaches have been explored. For example, specially designed structured substrates are used to deliver differentiated signals to each individual microrobots in a team [12]. A system is presented in [13] for simultaneous control of multiple magnetic microrobots based on the superposition of magnetic fields generated at centimeter-scale globally by electromagnetic coils as well as micrometer scale locally by microwires patterned on a glass substrate. Alternatively, all microrobots get the same global signal and respond distinctively due to their varying properties, e.g., mass, geometry, and magnetic hysteresis [14], [15]. Employing the fact that a swimmer obtains varying speed when it forms different angle with the applied rotating magnetic field, an autonomous controller was devised to manipulate two swimmers for independent and simultaneous waypoint-following tasks [16]. Distinct from these previous studies, Salehizadeh et al. used the local magnetic interactions between multiple agents, instead of neglecting these interactions and requiring that the agents are kept far apart, to control their positions [17]–[19]. Here, we utilize the same principle based on inter-agent forces to enable the localized control of two microgrippers in close proximity.

For the first time, this study presents a microrobtic multi-agent system that uses a single global magnetic field to independently and simultaneously actuate two untethered microgrippers in parallel to perform manipulation and transportation tasks. The two microgrippers are

This work is supported by the NSERC Discovery Grants Program.

J. Zhang, M. Salehizadeh, and E. Diller are with the department of Mechanical and Industrial Engineering, University of Toronto, 5 King's College Road, Toronto M5S 3G8, Canada ediller@mie.utoronto.ca

J. Zhang and M. Salehizadeh contributed equally to this work.

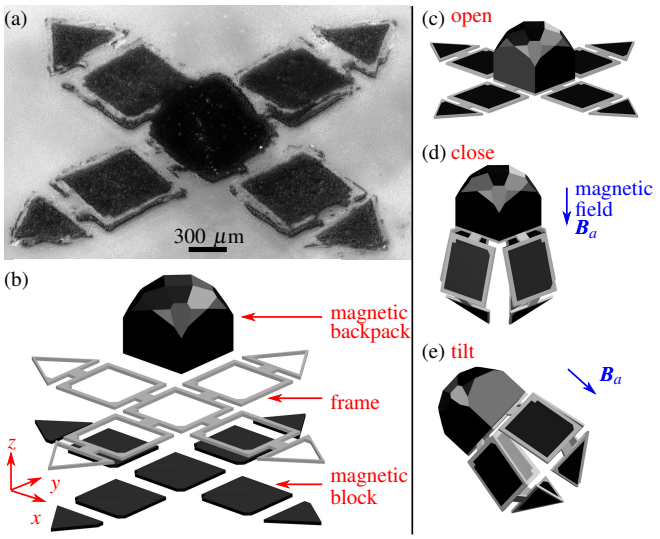


Fig. 1. The structure and working principles of the microgripper. The microgripper is shown in a composite photograph in (a) and further illustrated in an exploded drawing in (b). When magnetic field is absent, the microgripper remains open, see (c). The microgripper closes once a magnetic field is applied along its central axis, see (d). And its orientation is always aligned with the direction of the applied magnetic field, see (e).

independently positioned on a horizontal plane, utilizing both their local magnetic interactions and the forces and torques created by the global magnetic field. As a demonstration, two cargoes are picked up by two microgrippers and delivered to their respective destinations simultaneously along independent paths. The presented parallel operation of two microgrippers can potentially double the overall task efficiency and throughput. The utilization of inter-microgripper forces enables the two microgrippers to work in close proximity, which is often desired in cooperative teamworks. In future, a team of microgrippers can be potentially used for biopsy and loading/releasing drugs, while being navigated independently.

## II. Microgripper Concept

The microgrippers in this work are made of magnetic elastic polymers with embedded permanent magnetic microparticles. These microgrippers are similar to those in [5], [10] and explained briefly here. Each microgripper is centro-symmetric with nine magnetic blocks, one magnetic backpack, and one nonmagnetic frame that connects neighboring blocks, see Fig. 1(a) and (b). The blocks and backpack are made of polydimethylsiloxane (PDMS, Sylgard 184, Dow Corning) with embedded permanent magnetic microparticles (MQFP-15-7, NdPrFeB, Magnequench) at a 1:1 mass ratio. The implantation of magnetic microparticles increases the stiffness of the blocks and backpack, resulting in a Young's modulus between 1.45 and 2.23 MPa. On the other hand, the frame is made of a softer elastomer (Ecoflex0050, Smooth-On) with a nominal Young's modulus of 83 kPa. The combination of the relatively stiff blocks (as 'bones') and the relatively soft frame (as 'joint') makes the microgripper rigid enough to securely grasp cargoes and also flexible for easy closing and opening.

The magnetic microparticles make the microgripper magnetic responsive and fully controllable by a single global magnetic field. Specifically, the opening-and-closing, orientation, and position of the microgripper are dictated by the strength, direction, and spatiotemporal variance of the global magnetic field, respectively. When magnetic field is absent, the microgripper opens (3.5 mm tip-to-tip) due to the intrinsic elasticity of its polymeric material, see Fig. 1(c). The microgripper closes to form an approximate 700 $\mu$m sidewidth 3D box once a magnetic field is applied along its central axis, see Fig. 1(d). The orientation of the microgripper is always aligned with the direction of the global magnetic field due to magnetic torques, see Fig. 1(e). As a result, the microgripper can be rolled on a surface by rotating the global magnetic field. Alternatively, the microgripper can be pulled by magnetic forces in a nonuniform magnetic field. Different from our previous work, the microgripper here has an additional backpack, which has a magnetic moment along the microgripper central axis. The backpack is used to increase the net magnetic moment of the microgripper, in order to enhance the magnetic interactions between two microgrippers within the workspace. The microgripper is fabricated using standard photolithography and mold-replica techniques, and then magnetized in a uniform magnetic field of 1.1 T created by two permanent magnets.

## III. Two-Microgripper Control Scheme

This section explains the proposed control scheme for manipulating two microgrippers in parallel pick-and-place tasks. This controller consists of two layers: (1) a lower control layer including (i) a formation controller, (ii) a grasping sequence, and (iii) a releasing sequence; and (2) an upper control layer of a path planner.

### A. Lower Control Layer - Formation Controller

When two magnetic microgrippers are present in the same workspace, they exert magnetic forces and torques on each other via interactions of their local magnetic fields. In addition, both microgrippers experience magnetic forces and torques created by the global magnetic field, whose amplitude is set to be strong enough to override the local magnetic interactions between microgrippers. Two microgrippers are placed on a horizontal plane and the relevant parameters are defined in Fig. 2(a). This controller is similar to that in [17] and explained briefly here.

The microgrippers are always aligned with the global magnetic field $\boldsymbol{B}_a$, since the magnetic torques resulting from $\boldsymbol{B}_a$ are strong enough to override the one caused by the inter-microgripper magnetic interactions. Thus, both microgrippers have the same orientation angle $\psi_G$ with $\boldsymbol{B}_a$. The inter-microgripper forces control the separation $r = |\boldsymbol{r}_{12}|$ and the heading $\phi$ of the microgripper pair, while the magnetic forces created by $\nabla \boldsymbol{B}_a$ pull the microgripper pair around and thus change the position of its center-of-mass

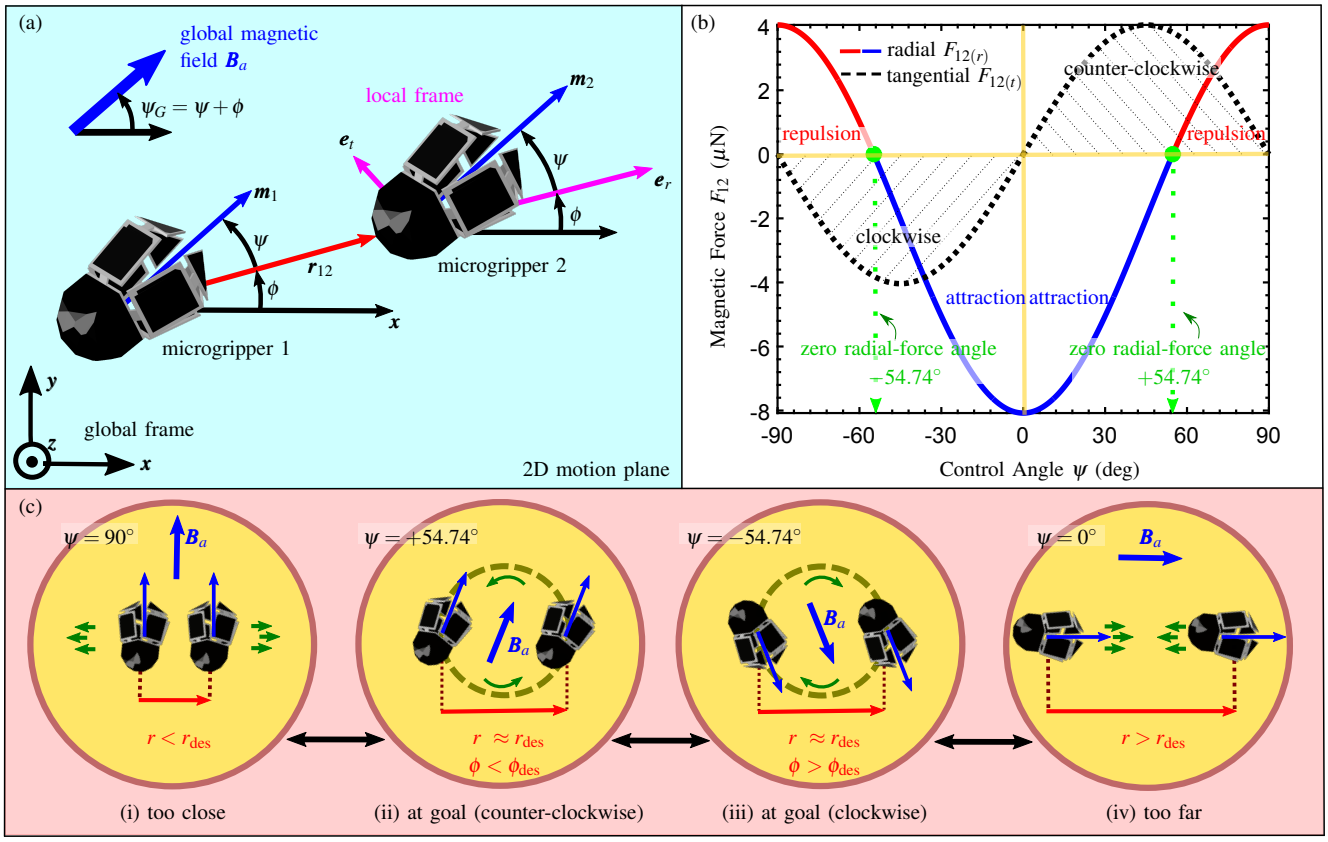


Fig. 2. The principles of the localized control of two microgrippers on a horizontal plane. The definitions of relevant parameters are given in (a) in both a global and a local coordinate frames. The two-microgripper separation vector pointing from microgripper 1 to 2 and the pair heading are denoted by $\boldsymbol{r}_{12}$ and $\phi$, respectively. The radial and tangential coordinates are shown by $\boldsymbol{e}_r$ and $\boldsymbol{e}_t$. The control input is the angle that the magnetizations make with the radial axis in the motion plane shown by $\psi$. The radial and tangential components of the interactive magnetic force between two microgrippers are plotted in (b) versus $\psi$ by solid and dashed lines, respectively. $r = 5R$ ($R$ denotes the agent nominal radius). (c) States of microgripper attraction or repulsion as well as pair heading rotation are determined by the direction and sign of the global magnetic field $\boldsymbol{B}_a$, respectively: i) repulsion at $\psi = 90°$, ii) zero radial-force at $\psi = +54.74°$ with counter-clockwise rotation, iii) zero radial-force at $\psi = -54.74°$ with clockwise rotation, iv) attraction at $\psi = 0°$.

$P_{\text{com}}$. Ultimately, the two microgrippers are independently and simultaneously positioned on a horizontal plane using both the global magnetic field $\boldsymbol{B}_a$ and the inter-microgripper magnetic interactions.

Since the inter-microgripper magnetic torques are overridden by the torques produced by the global magnetic field $\boldsymbol{B}_a$, we only study the magnetic forces in the local interaction between the two microgrippers (see [17] for details on the minimum separation and field requirement). Here, the microgrippers are considered as magnetic dipoles. Let $\boldsymbol{B}_{12}$ represent the magnetic flux density at the position of microgripper 2 with magnetic moment $\boldsymbol{m}_2$ created by microgripper 1 with magnetic moment $\boldsymbol{m}_1$. From the magnetic dipole model, there is

$$\boldsymbol{B}_{12} = \frac{\mu_0}{4\pi r^3}\left(\frac{3(\boldsymbol{m}_1 \cdot \boldsymbol{r}_{12})\boldsymbol{r}_{12}}{r^2} - \boldsymbol{m}_1\right), \tag{1}$$

where $\mu_0 = 4\pi \times 10^{-7}$ H/m is the vacuum permeability. The magnetic field gradient $\nabla \boldsymbol{B}_{12}$ creates a force $\boldsymbol{F}_{12}$ on microgripper 2, which is

$$\boldsymbol{F}_{12} = \nabla(\boldsymbol{m}_2 \cdot \boldsymbol{B}_{12}). \tag{2}$$

At the same time, a counterforce $\boldsymbol{F}_{21} = -\boldsymbol{F}_{12}$ applies on microgripper 1. Substituting Eq. (1) into Eq. (2), the radial and the tangential components of $\boldsymbol{F}_{12}$ are written in the local Cartesian coordinates ($\boldsymbol{e}_r$, $\boldsymbol{e}_t$) as

$$F_{12(r)} = \frac{3\mu_0 m_1 m_2}{4\pi r_{12}^4}\left(1 - 3\cos^2\psi\right) \tag{3}$$

and

$$F_{12(t)} = \frac{3\mu_0 m_1 m_2}{4\pi r_{12}^4}\sin(2\psi), \tag{4}$$

respectively. $\psi$ is the local in-plane control input angle defined as the angle between the global magnetic field $\boldsymbol{B}_a$ and $\boldsymbol{r}_{12}$ in the motion plane, see Fig. 2(a).

The values of $F_{12(r)}$ and $F_{12(t)}$ are plotted in Fig. 2(b) with respect to the control angle $\psi$. Similarly, $\psi_G = \psi + \phi$ is the in-plane control angle in the global coordinate frame. From this figure, one can develop a radial proportional controller (P-controller) for the modulation of the inter-microgripper magnetic force as a function of the control angle $\psi$ [17]. At $\psi = 0°$ and $\psi = \pm 90°$ the radial force attains its maximum attractive (negative) and repulsive (positive) value, respectively. Consequently as demonstrated in Fig. 2(c), when two agents are too close with respect to the desired separation ($r < r_{\text{des}}$), the controller will be saturated by

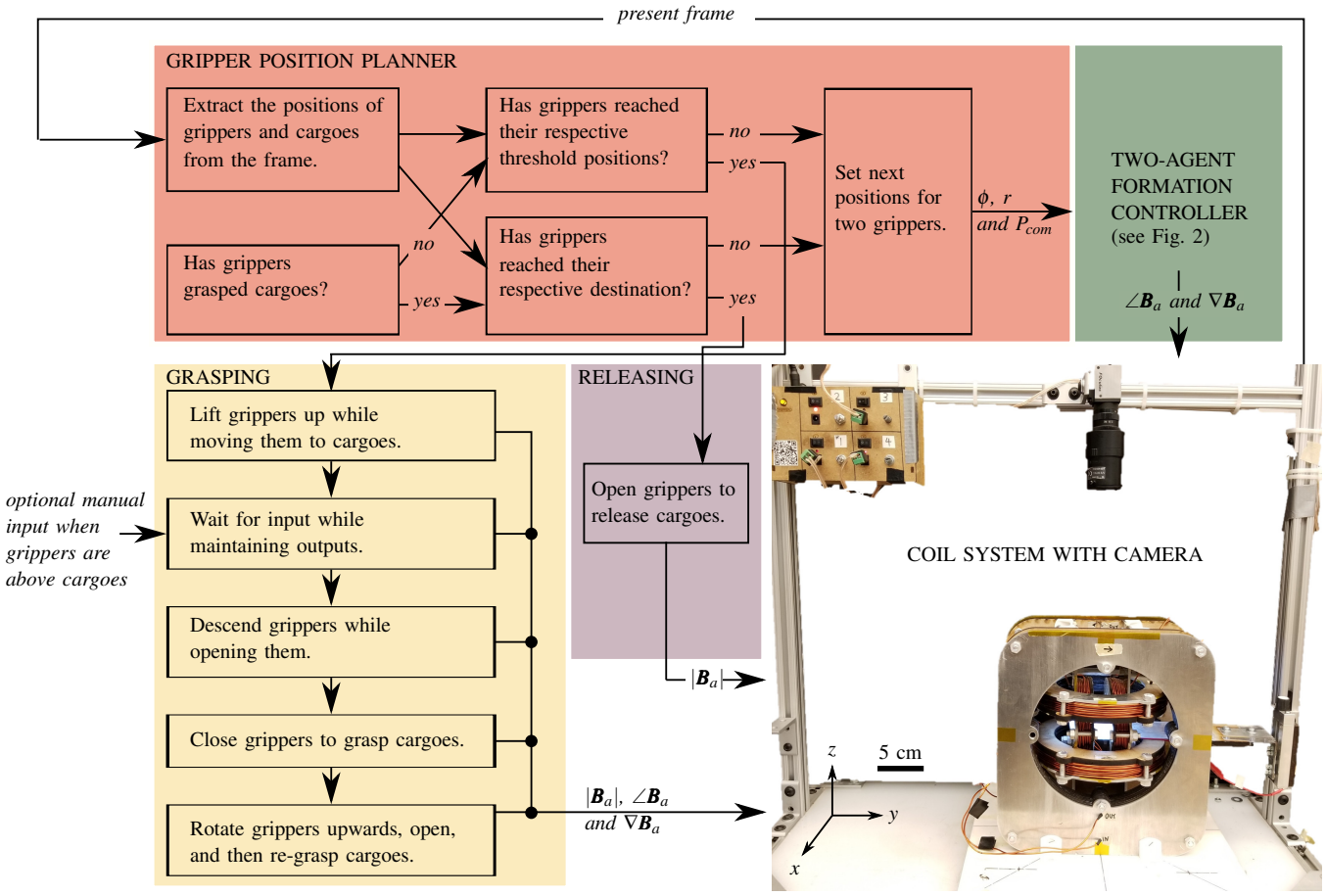


Fig. 3. Structure of the proposed two-microgripper controller scheme. After initialization, the controller extracts the present position information of the microgrippers and cargoes from real-time top-view camera frames. Then, the planner decides to whether keep moving microgrippers closer to their respectively goals, or proceed into an action of grasping or releasing cargoes. The decision made by the controller is ultimately implemented by the coil system, whose peripheral power suppliers and amplifiers are not shown in the photograph for better visibility.

pointing the field orientation perpendicular to their separation vector $\boldsymbol{r}$ so that agents repel each other with full radial force. If two agents are too far ($r > r_{\text{des}}$), the controller will be saturated by orienting the field parallel to their separation vector $\boldsymbol{r}$ so that agents attract each other with full radial force. Importantly, at $\psi = 54.74^\circ$ the radial force becomes zero. If the space between two agents is around the goal spacing ($r \approx r_{\text{des}}$), the controller would choose intermediate angles between $0^\circ$ and $90^\circ$ centered around the setpoint angle $\psi_s = 54.74^\circ$, leading to the P-control law: $\psi = \psi_s - K\|\varepsilon_r\|$ where the radial separation error is denoted by $\varepsilon_r = r - r_{\text{des}}$ and $K$ represents the control gain. It can be seen from Fig. 2(b) that at any angle between 0 and $90^\circ$, a non-zero tangential force occurs which causes the pair of microgrippers to rotate about one another. Also by reflecting the control angle about $\psi = 0^\circ$, the tangential force can be reversed without affecting the radial force. This sign flipping enables the control of the pair heading $\phi$ around its goal $\phi_{\text{des}}$ by constantly switching the rotation direction of the pair complex as represented in the state transition of Fig. 2(c).

The formation controller explained in this subsection controls a 3D electromagnetic coil system through a DAQ I/O board (Model 826, Sensoray). The formation controller acts as one part of the lower layer of the proposed control scheme, see Fig. 3.

### *B. Lower Control Layer - Grasping and Release Sequence*

Once both microgrippers have reached their designated positions, i.e., the threshold positions or destinations, a sequence of open-loop actions will be implemented to make the microgrippers grasp or release their respective cargoes. For grasping, the microgrippers are first lifted up and pulled towards the top of cargoes by applying magnetic field gradient. Lifting the microgrippers is necessary because the cargoes will be pushed away or aside if the microgrippers move directly to the cargoes at the same plane.

When both microgrippers are right above their respective cargoes, the global magnetic field $\boldsymbol{B}_a$ is removed and then the microgrippers open and descend at the same time. The timing of this action can be decided by setting a fixed time period, automatic tracking from optical feedback, or manual monitoring, which is used in this work as a proof-of-concept. The microgrippers are then closed by restoring the magnetic field $\boldsymbol{B}_a$ without field gradient. Next, a re-grasping action is performed to ensure the microgrippers securely grasp their cargoes and will not lose them during transportation. On the

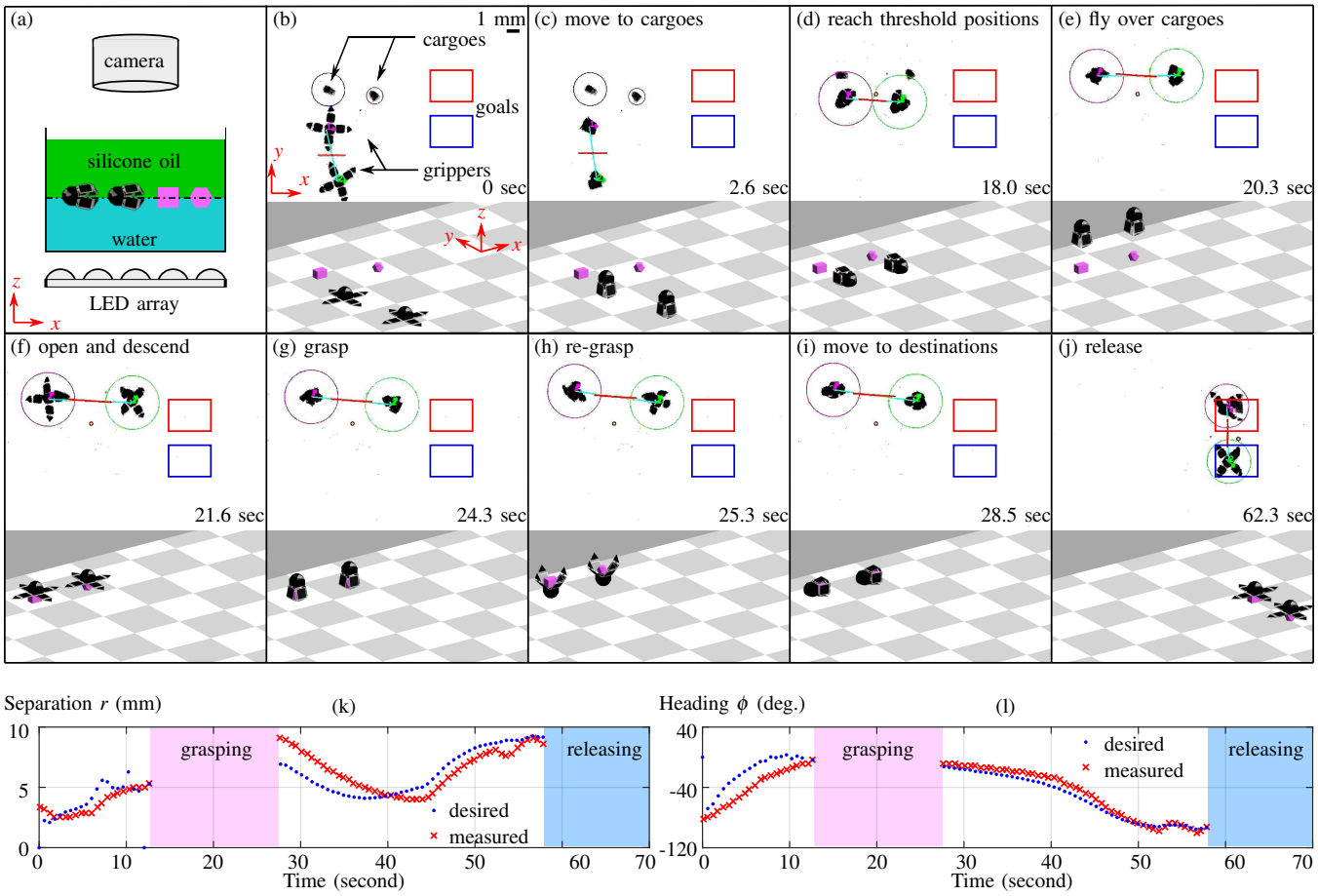


Fig. 4. Experimental setup and results of two microgrippers picking and placing cargoes. Two microgrippers and two cargoes are placed at the interface between water and silicone oil, which is illuminated by a LED array and monitored by a top-view camera, see (a). A sequence of top-view frames of the workspace is shown chronologically in (b)-(j), together with their respective 3D renderings. The desired separation $r$ and heading $\phi$ values of the microgripper pair are plotted in (k) and (l), respectively, together with the corresponding measured values. Video is available in supplementary materials.

other hand, the releasing sequence is simply removing the magnetic field $\boldsymbol{B}_a$ and the microgrippers will open to release cargoes to their current positions.

### C. Upper Control Layer - Path Planner

The upper layer of the scheme processes the feedback information and decides the next action. A schematic of the scheme is illustrated in Fig. 3. The upper layer extracts the present positions of the microgrippers and cargoes from the optical feedback, i.e., the frames captured by a top-view camera in real time, using a contour-finding algorithm from the OpenCV library. Then the path planner uses the position information to calculate the next desired positions for the two microgrippers. The path planner activates the formation controllers in the lower layer, if the microgrippers have not reached the designated positions, i.e., the threshold positions for grasping or the destinations for releasing. The path planner processes the position information in the global $xy$ coordinate, and convert it into the $(r, \phi, P_{\text{com}})$ coordinate so that the formation controller recognizes it. Alternatively, if both microgrippers have reached their respective designated positions, the path planner chooses between the grasping sequence or the releasing sequence based on whether or not the microgrippers have grasped cargoes.

Overall, the upper layer path planner monitors the positions of the microgrippers and cargoes and decides the next action of the microgrippers. On the other hand, the lower layer receives the information from the upper layer and set appropriate global magnetic field $\boldsymbol{B}_a$ to realize the request.

## IV. Experimental Results

To demonstrate the efficacy of the proposed control scheme, two microgrippers are placed at an interface between water and silicone oil (25 cSt), see Fig 4(a), and positioned independently and simultaneously to pick-and-place two cargoes, respectively. A sequence of frames captured during this experiment is shown in Fig. 4(b)-(j).

In this experiment, the two microgrippers are initially aligned with $+y$ axis, while the two cargoes are aligned with $+x$ axis, see Fig. 4(b). The controller manipulates both microgrippers towards their respective cargoes until they reach the threshold positions, which are a certain distance away but parallel with the cargoes, see Fig. 4(c) and (d). During this process, the threshold positions are updated in real time by the controller since the cargoes drift away due to the microgrippers' movements. Next, the microgrippers

are lifted up and towards the cargoes by the magnetic forces created by the global magnetic field gradient, see Fig. 4(e). Microgrippers are lifted in order to avoid disturbing cargoes in close proximity and therefore make grasping easier. Once the microgrippers are above the cargoes, a manual input triggers the controller to remove the global magnetic field. As a result, both microgrippers open and descend, landing on the cargoes, see Fig. 4(f). In the following step, the microgrippers close to grasp cargoes, rotate from $-z$ to $+z$, open, and then close again, see Fig. 4(g) and (h). This procedure lets the cargoes, which are originally grasped by the tips of the microgrippers, fall into the hug of the microgrippers for secure grasping, reducing the possibility of losing cargoes during the following transportation. Finally, the two microgrippers move to their respective destinations and release cargoes there, see Fig. 4(i) and (j).

During this experiment, the path planner processes the position information in the global $(x, y)$ coordinate, while the formation controller operates on the $(r, \phi, P_{\text{com}})$ coordinate. The desired and measured values of the separation $r$ and heading $\phi$ of the microgripper pair are plotted in Fig 4(k) and (l), respectively. It is obvious that the measured values tightly follow the desired value with a small time delay. There is a relatively large time delay between the desired and the measured separation $r$ after the grasping sequence. The reason is that the two microgrippers are far away from each other and their interactive force is weak, see Fig. 2(b), causing them to move slowly and elongating the time delay.

## V. Conclusions

This work presents the first example of controlling two untethered mobile microgrippers in parallel using a single global input for independent positioning and synchronal picking-and-placing cargoes, based on the global and local magnetic interactions between the two microgrippers and a global magnetic field. An experiment demonstrates that this controller simultaneously manipulates two microgrippers to pick up two cargoes and deliver them to their respective destinations. This work pioneers the control of multiple microgrippers using global inputs for teamwork tasks. Deploying multiple microgrippers in a task could potentially boost the throughput and enable jobs that cannot be achieved by a single agent. The two 3D microgrippers configuration is intuitive in teleoperations, since it imitates the two-hand case of human beings. Thus, this work exhibits promising applications in cell manipulation and microassembly. Moreover, using global inputs is usually easier to implement and control than deploying localized inputs for each individual in a team. In this work, the two microgrippers are mostly constrained to an interface of water and silicone oil, because the coil system cannot compensates their gravities and exerts controls at the same time. In future research, microgrippers of lower density values and smaller sizes will be fabricated using low-density polymers and hollow glass microbeads, and the capability of freely moving microgrippers in the 3D space will be explored. The deployed formation controller also works with more than two agents, see [19]. Thus, controlling three or more microgrippers will be explored in future work. Moreover, a more sophisticated path planner will be devised to manipulate microgrippers to follow specified trajectories and avoid obstacles.

## References


[1] A. Ghosh, C. Yoon, F. Ongaro, S. Scheggi, F. Selaru, S. Misra, and D. Gracias, "Stimuli-responsive soft untethered grippers for drug delivery and robotic surgery," *Front. Mech. Eng.*, vol. 3, p. 7, 2017.

[2] C. Iss, G. Ortiz, A. Truong, Y. Hou, T. Livache, R. Calemczuk, P. Sabon, E. Gautier, S. Auffret, L. Buda-Prejbeanu, N. Strelkov, H. Joisten, and B. Dieny, "Fabrication of nanotweezers and their remote actuation by magnetic fields," *Sci. Rep.*, vol. 7, no. 1, p. 451, 2017.

[3] N. Inomata, T. Mizunuma, Y. Yamanishi, and F. Arai, "Omnidirectional actuation of magnetically driven microtool for cutting of oocyte in a chip," *J. Microelectromech. Syst.*, vol. 20, no. 2, pp. 383–388, 2011.

[4] J. Randhawa, T. Leong, N. Bassik, B. Benson, M. Jochmans, and D. Gracias, "Pick-and-place using chemically actuated microgrippers," *J. Am. Chem. Soc.*, vol. 130, no. 51, pp. 17 238–17 239, 2008.

[5] J. Zhang and E. Diller, "Tetherless mobile micrograsping using a magnetic elastic composite material," *Smart Mater. Struct.*, vol. 25, no. 11, p. 11LT03, 2016.

[6] T. Leong, C. Randall, B. Benson, N. Bassik, G. Stern, and D. Gracias, "Tetherless Thermobiochemically Actuated Microgrippers," *Proc. Natl. Acad. Sci. U.S.A.*, vol. 106, no. 3, pp. 703–708, 2009.

[7] C. Pacchierotti, F. Ongaro, F. Van den Brink, C. Yoon, D. Prattichizzo, D. H. Gracias, and S. Misra, "Steering and control of miniaturized untethered soft magnetic grippers with haptic assistance," *IEEE Trans. Autom. Sci. Eng.*, vol. PP, no. 99, pp. 1–17, 2017.

[8] S. Scheggi, K. K. T. Chandrasekar, C. Yoon, B. Sawaryn, G. van de Steeg, D. H. Gracias, and S. Misra, "Magnetic motion control and planning of untethered soft grippers using ultrasound image feedback," in *IEEE Int. Conf. Robot. Autom.*, 2017, pp. 6156–6161.

[9] S. Chowdhury, W. Jing, and D. J. Cappelleri, "Controlling multiple microrobots: recent progress and future challenges," *J. Micro-Bio Robot.*, vol. 10, no. 1, pp. 1–11, 2015.

[10] J. Zhang, O. Onaizah, K. Middleton, L. You, and E. Diller, "Reliable grasping of three-dimensional untethered mobile magnetic microgripper for autonomous pick-and-place," *IEEE Robot. Autom. Lett.*, vol. 2, no. 2, pp. 835–840, 2017.

[11] S. Yim, E. Gultepe, D. Gracias, and M. Sitti, "Biopsy using a magnetic capsule endoscope carrying, releasing, and retrieving untethered microgrippers," *IEEE Trans. Biomed. Eng.*, vol. 61, no. 2, pp. 513–521, 2014.

[12] S. Chowdhury, B. V. Johnson, W. Jing, and D. J. Cappelleri, "Designing local magnetic fields and path planning for independent actuation of multiple mobile microrobots," *J. Micro-Bio Robot.*, vol. 12, no. 1, pp. 21–31, 2017.

[13] E. Steager, D. Wong, J. Wang, S. Arora, and V. Kumar, "Control of multiple microrobots with multiscale magnetic field superposition," in *Int. Conf. Manipulation, Automation and Robotics at Small Scales*, 2017, pp. 1–6.

[14] A. Becker, Y. Ou, P. Kim, M. J. Kim, and A. Julius, "Feedback control of many magnetized: Tetrahymena pyriformis cells by exploiting phase inhomogeneity," in *IEEE/RSJ Int. Conf. Intell. Robots Syst.*, 2013, pp. 3317–3323.

[15] S. Miyashita, E. Diller, and M. Sitti, "Two-dimensional magnetic micro-module reconfigurations based on inter-modular interactions," *Int. J. Robot. Res.*, vol. 32, no. 5, pp. 591–613, 2013.

[16] J. Zhang, P. Jain, and E. Diller, "Independent control of two millimeter-scale soft-bodied magnetic robotic swimmers," in *IEEE Int. Conf. Robot. Autom.*, 2016, pp. 1933–38.

[17] M. Salehizadeh and E. Diller, "Two-agent formation control of magnetic microrobots," in *Int. Conf. Manipulation, Automation and Robotics at Small Scales*, 2016, pp. 1–6.

[18] M. Salehizadeh and E. Diller, "Two-agent formation control of magnetic microrobots in two dimensions," *J. Micro-Bio Robot.*, vol. 12, no. 1, pp. 9–19, 2017.

[19] M. Salehizadeh and E. Diller, "Optimization-based formation control of underactuated magnetic microrobots via inter-agent forces," in *Int. Conf. Manipulation, Automation and Robotics at Small Scales*, 2017, pp. 1–5.